Computational Structural Engineering
An International Journal
Vol. 2, No. 1, pp. 43~50 (2002)

Computational Structural Engineering Institute

Dynamic Wave Response Analysis of Floating Bodies in the Time-domain

Eiichi Watanabe†, Tomoaki Utsunomiya and Nao Yoshizawa

Department of Civil Engineering, Kyoto University, Kyoto 606-8501, Japan

Received June 2002; Accepted October 2002

ABSTRACT

This paper presents a method to predict dynamic responses of floating bodies in the time domain. Because of the frequency-dependence of the radiation wave forces, the memory effect must be taken into account when the responses are evaluated in the time domain. Although the formulations firstly developed by Cummins (1962) have been well-known for this purpose, the effective numerical procedure has not been established yet. This study employs FFT (Fast Fourier Transform) algorithm to evaluate the memory effect function, and the equations of motion of an integro-differential type are solved by Newmark-β method. Numerical examples for a truncated circular cylinder have indicated the effectiveness of the proposed numerical procedure.

Keywords: floating body, memory effect function, wave response, time domain analysis, fast fourier transform, newmark-β method

1. Introduction

The mooring method is one of the key factors for floating structures such as floating bridges (see for example, Lwin, 2000; Maruyama *et al.*, 1998). The methods by such as chain and dolphin with rubber fenders have been adopted. In view of the fact, however, that these mooring systems exhibit the nonlinearity in the restoring force characteristics, the response of the floating structure becomes nonlinear under the wind or wave loadings. Apparently, the response analysis in the frequency domain is not possible and the time series analysis is required instead. On the other hand, in the hydrodynamic analysis, the hydrodynamic matrices have terms depending on the frequency and consequently, the response analysis should take into account the memory effect of the hydrodynamic forces as in the references (Cummins, 1962; Takagi and Arai, 1996). Although the computer programs have been developed by several researchers (Maeda *et al.*, 1991; Endo and Yago, 1999; Kashiwagi, 2000), the effective numerical procedure has not been established yet.

This study has employed FFT (Fast Fourier Transform) algorithm to calculate the memory effect functions, and Newmark-β method (Newmark, 1959) to solve equations of motion in the time domain. The FFT in the calculation of memory effect functions has successfully been implemented as can be seen in the numerical examples. The Newmark-β method, by which the nonlinear restoring force characteristics can be easily handled, has also been successfully used in this study. In order to demonstrate the validity of the developed program herein, numerical examples for a single truncated circular cylinder, for which the published results are available, are shown.

Newman (1985) has treated the time series free oscillation analysis of a floating cylinder of a single D.O.F. (Heaving Motion) in the case of infinite depth water. Since this heaving motion is the most fundamental problem to start with, a new computer program is developed and the results are compared with those by Newman (1985). Then, the program is extended to consider the forced oscillations either to regular or irregular random waves and the accuracy is evaluated. This program is further extended to higher D.O.F., namely, 3 D.O.F. (surging, heaving and pitching) and the necessary accuracy checks are conducted.

2. Equations of Motion and Numerical Procedure

The equations of motion of a single floating body subjected to time-dependent external wave forces can be rep-

† Corresponding author
Tel. +81-75-753-5077; Fax: +81-75-753-5130
E-mail address: watanabe@str.kuciv.kyoto-u.ac.jp

resented as follows (Cummins, 1962):

$$\sum_{j=1}^{6}[\{m_{ij}+\mu_{ij}(\infty)\}\ddot{\zeta}_j(t)+\int_0^{\infty}L_{ij}(\tau)\ddot{\zeta}_j(t-\tau)d\tau+K_{ij}\zeta_j(t)]=F_i(t)$$
$$(i=1,2,\ldots,6) \tag{1}$$

where m_{ij} refers to the mass matrix of the floating body, $L_{ij}(t)$ the static restoring force coefficient matrix, $F_i(t)$ the external time-dependent force vector, $\mu_{ij}(\infty)$ the added mass matrix at infinite frequency, $\zeta_j(t)$ the motion vector of the floating body, and $\ddot{\zeta}_j(t)$ the acceleration vector. $L_{ij}(t)$ is referred to as the memory effect function matrix, which represents part of the radiation wave forces influenced by the past response of the floating body. The indexes $i = 1,2,3$ correspond to the forces in the directions of x,y,z, respectively, and $i = 4,5,6$ correspond to the moments around the x-axis, y-axis, z-axis, respectively. Similarly, $j = 1,2,3$ correspond to the translation motions in the directions of x (surge), y (sway), z (heave), respectively, and $j = 4,5,6$ correspond to the rotations around the x-axis (roll), y-axis (pitch), z-axis (yaw), respectively.

The memory effect function $L_{ij}(t)$ can be computed by the following equation:

$$L_{ij}(t)=\frac{2}{\pi}\int_0^{\infty}\sin\ \omega t\frac{\lambda_{ij}(\omega)}{\omega}d\omega \tag{2}$$

where $\lambda_{ij}(\omega)$ is the radiation damping coefficient matrix of frequency dependent.

The added-mass matrix at infinite frequency $\mu_{ij}(\infty)$ may be calculated by the following relationship:

$$\mu_{ij}(\omega_1)-\mu_{ij}(\infty)=\frac{2}{\pi}P.V.\int_0^{\infty}\lambda_{ij}(\omega)\frac{d\omega}{\omega_1^2-\omega^2} \tag{3}$$

where $\mu_{ij}(\omega)$ is the added-mass matrix of frequency dependent, and P.V. represents principal value.

In order to obtain the memory effect function $L_{ij}(t)$ and the added-mass matrix at infinite frequency $\mu_{ij}(\infty)$, we firstly calculate the added-mass matrix $\mu_{ij}(\omega)$ and the radiation damping coefficient matrix $\lambda_{ij}(\omega)$ in the frequency domain. In this study, we have calculated these values by the eigen-function expansion matching method for a truncated circular cylinder located in the finite depth water, because of the computational efficiency (Yeung, 1981). For floating bodies having general shape located in the finite or infinite depth water, we have calculated those values by the higher order boundary element method (HOBEM) employing the free surface Green's function (Teng and Eatock Taylor, 1995).

Former studies (Maeda *et al.*, 1991; Endo and Yago, 1999; Kashiwagi, 2000) have evaluated the memory effect function $L_{ij}(t)$ by direct numerical integration of Eq. (2); however, such a direct numerical evaluation requires excessive computation time, as pointed out by Kashiwagi (2000). In stead, we have employed FFT algorithm to compute the memory effect function $L_{ij}(t)$ by the inverse Fourier sine transform of $\lambda_{ij}(\omega)/\omega$ as indicated in Eq. (2). The interval of the integration is approximated to be between $\omega = 0$ and $\omega = \omega_{\max}$, and the interval is equally divided into $N+1$ portions with the same interval of $\Delta\omega = \omega_{\max}/(N+1)$. Then, Eq. (2) can be approximated by using the discrete inverse Fourier sine transform and assuming $t = m\Delta t$, where $\Delta t = \pi/\omega_{\max}$, as

$$L_{ij}(m\Delta t)=\frac{2}{\pi}\Delta\omega\sum_{n=1}^{N}\sin\left(\frac{mn\pi}{N+1}\right)\frac{\lambda_{ij}(n\Delta\omega)}{n\Delta\omega}\quad(m=1,2,K,N+1) \tag{4}$$

The calculation of Eq. (4) can be made very efficiently with the computation time of $O(N \log N)$ using a FFT subroutine program (DFSINT in IMSL subroutine package, for example).

The time-domain numerical simulation program has been developed based on the Newmark-β method. A brief description of the algorithm in a general form is shown as follows:

$$[M]\{\ddot{\zeta}(t)\}+[C]\{\dot{\zeta}(t)\}+[K]\{\zeta(t)\}=\{F(t)\} \tag{5}$$

$$\{\ddot{\zeta}(t+\Delta t)\}=([M]+(\Delta t/2)[C]+\beta(\Delta t)^2[K])^{-1}$$
$$\left[\{F(t+\Delta t)\}-[C](\{\dot{\zeta}(t)\}+\frac{\Delta t}{2}\{\ddot{\zeta}(t)\}\right.$$
$$\left.-[K](\{\zeta(t)\}+\Delta t\{\dot{\zeta}(t)\}+\left(\frac{1}{2}-\beta\right)(\Delta t)^2\{\ddot{\zeta}(t)\})\right] \tag{6}$$

$$\{\dot{\zeta}(t+\Delta t)\}=\{\zeta(t)\}+(\Delta t/2)(\{\ddot{\zeta}(t)\}+\{\ddot{\zeta}(t+\Delta t)\}) \tag{7}$$

$$\{\zeta(t+\Delta t)\}=\{\zeta(t)\}+\frac{\Delta t}{1!}\{\dot{\zeta}(t)\}+\frac{(\Delta t)^2}{2!}\{\ddot{\zeta}(t)\}$$
$$+\beta(\Delta t)^3\frac{\{\ddot{\zeta}(t+\Delta t)\}-\{\ddot{\zeta}(t)\}}{\Delta t} \tag{8}$$

where $[M]$ represents mass matrix, $[C]$ damping coefficient matrix, $[K]$ restoring force coefficient matrix, $\{F(t)\}$ the external force vector, and $\{\zeta(t)\}$ the response displacement of the floating body. Solving Eqs. (6)-(8) for each time step, we obtain the time series response of $\{\zeta(t)\}$. In this study, we use $\beta = 1/4$ for its numerical stability (Newmark, 1959).

3. Analysis of Free Heaving Oscillation

Free heaving oscillation of the truncated circular cylinder located in the infinite depth sea has been analyzed. In the following, all quantities are non-dimensionalized in terms of the radius of the cylinder a, the gravity acceleration g and the density of the fluid ρ as summarized in Table 1. Fig. 1 shows the analytical model. It has the radius $a = 1.0$ and the draft $D = 0.5$.

Table 1. Non-dimensional parameters (^: dimensional parameters)

Time	$t = \hat{t}\sqrt{\frac{\hat{g}}{\hat{a}}}$
Circular frequency	$\omega = \hat{\omega}\sqrt{\frac{\hat{a}}{\hat{g}}}$
Force	$F = \frac{\hat{F}}{\hat{\rho}\hat{g}\hat{a}^3}$
Moment	$M = \frac{\hat{M}}{\hat{\rho}\hat{g}\hat{a}^4}$
Mass	$m = \frac{\hat{m}}{\hat{\rho}\hat{a}^3}$
Restoring force coefficient	$K_{11} = \frac{\hat{K}_{11}}{\hat{\rho}\hat{g}\hat{a}^2}$, $K_{33} = \frac{\hat{K}_{33}}{\hat{\rho}\hat{g}\hat{a}^2}$, $K_{55} = \frac{\hat{K}_{55}}{\hat{\rho}\hat{g}\hat{a}^4}$
Displacement	$\zeta = \frac{\hat{\zeta}}{\hat{a}}$
Velocity	$\dot{\zeta} = \frac{\dot{\hat{\zeta}}}{\hat{a}}\sqrt{\frac{\hat{a}}{\hat{g}}}$
Acceleration	$\ddot{\zeta} = \frac{\ddot{\hat{\zeta}}}{\hat{g}}$
Added mass	$\mu = \frac{\hat{\mu}}{\hat{\rho}\hat{a}^3}$
Radiation damping coefficient	$\lambda = \frac{\hat{\lambda}}{\hat{\rho}\hat{a}^3}\sqrt{\frac{\hat{a}}{\hat{g}}}$
Memory effect function	$L = \frac{\hat{L}}{\hat{\rho}\hat{a}^3}\sqrt{\frac{\hat{a}}{\hat{g}}}$
Power spectrum of wave	$S_0 = \frac{\hat{S}_0}{\hat{a}^2}\sqrt{\frac{\hat{g}}{\hat{a}}}$
Power spectrum of wave force	$S_0 = \frac{\hat{S}}{\hat{\rho}^2\hat{a}^3\hat{g}}\sqrt{\frac{\hat{g}}{\hat{a}}}$

When the initial conditions are given by $\zeta_3(0) = 0$ and $\dot{\zeta}_3(0) = 1$, then the equation of the heaving motion can be expressed by the following equation:

$$\{m_{33}+\mu_{33}(\infty)\}\ddot{\zeta}_3(t)+\int_0^t L_{33}(\tau)\ddot{\zeta}_3(t-\tau)d\tau+L_{33}(t) +K_{33}\zeta_3(t) = 0 \quad (9)$$

where $m_{33} = \pi a^2 D = 0.5\pi$ and $K_{33} = \rho g \pi a^2 = \pi$ when non-dimensional quantities are used. Furthermore, the added-mass at the infinite frequency is given by Newman (1985) as $\mu_{33}(\infty) = 1.7414$ when $D = 0.5$. By moving the 3rd and 4th terms of the left-hand side of Eq. (9) to the right-hand side, and considering them as the external force $F_3(t)$, Eq. (9) becomes identical to Eq. (5), and thus can be solved by Eqs. (6)-(8).

Fig. 2 shows the evaluation of $L_{33}(t)$ by the proposed method and its comparison with the one by Newman (1985). When the value of t becomes larger, such as

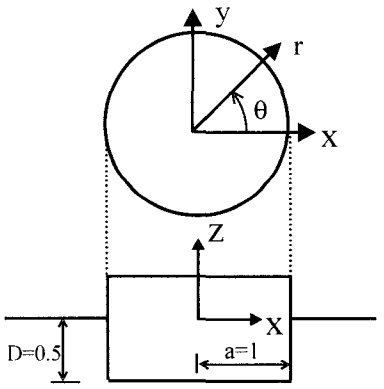

Fig. 1. Configuration of the analyzed model.

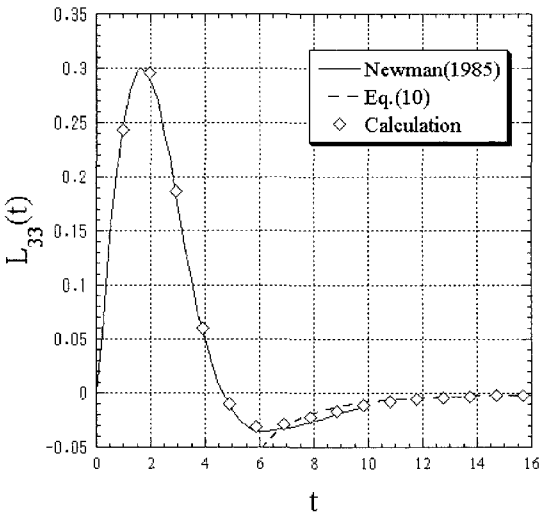

Fig. 2. Memory effect function.

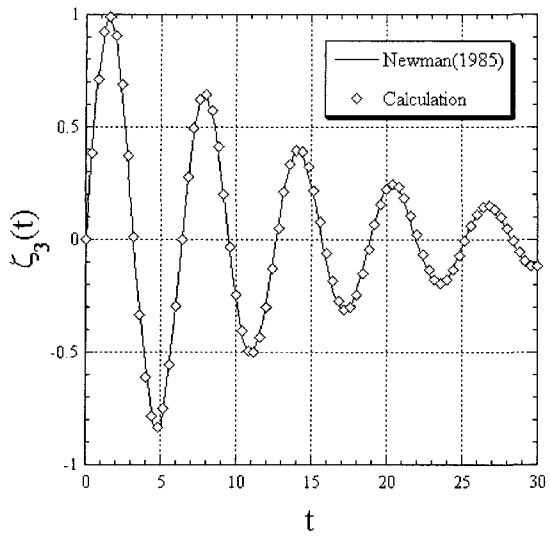

Fig. 3. Free heaving oscillation.

$t>10$, $L_{33}(t)$ will become very close to the following asymptotic equation:

$$L_{33}(t)\approx -2\pi t^{-3}-(24\pi+48\mu_{33}(0))t^{-5} \qquad (10)$$

where $\mu_{33}(0) = 2.3775$. As can be seen in Fig. 2, the results by the present study agree well with Eq. (10) when $t>10$ and with the graph plot in Newman (1985) when $t\le 10$. Therefore, the calculation method for the memory effect function using FFT has been verified.

Fig. 3 shows the heaving response $\zeta_3(t)$ by the proposed method, and its comparison with the one by Newman (1985). Again, satisfactory agreement is observed, thus confirming the validity of the proposed numerical method. Theoretically, the memory effect function $L_{33}(t)$ has to be integrated over the entire analyzed duration (from $\tau = 0$ to $\tau = t$) as defined in Eq. (9). However, in the actual computation, the integration has been made up to $\tau = 16$ when $t\ge 16$, based on the approximation that $L_{33}(t) = 0$ for $t\ge 16$ (see Fig. 2).

4. Analysis of Heaving Motion in Waves

In general, the heaving oscillation of a freely floating body can be analyzed as 1 D.O.F. system. The heaving motion in waves has thus been analyzed as the same 1 D.O.F. system as in the previous section. The analytical model is again the truncated circular cylinder with $a = 1$ and $D = 0.5$, but the constant water depth is assumed to be $h = 10.0$.

4.1 Evaluation of Memory Effect Function and Added-mass at Infinite Frequency

Firstly, the memory effect function $L_{33}(t)$ and the added-mass at infinite frequency $\mu_{33}(\infty)$ are evaluated by Eqs. (2) and (3). The memory effect function $L_{33}(t)$ has been evaluated by the same procedure using the FFT algorithm as given in Section 3. The added-mass at infinite frequency $\mu_{33}(\infty)$ has been calculated using Eq. (3) from the added-mass $\mu_{33}(\omega_i)$ at some particular frequencies and the radiation damping coefficient $\lambda_{33}(\omega)$.

The memory effect function $L_{33}(t)$ is computed from the inverse Fourier transform of $\lambda_{33}(\omega)/\omega$ as shown in Fig. 4 for different number of the division $N = 32, 256, 1024$ of the interval $0\le\omega\le 2\pi$. For $\omega\ge 2\pi$, the value of

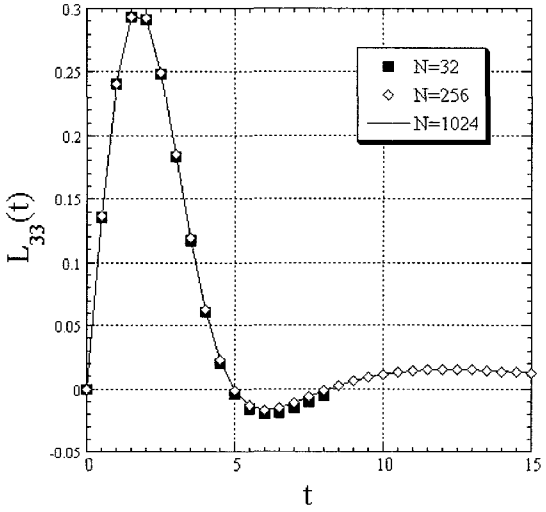

Fig. 4. Memory effect function.

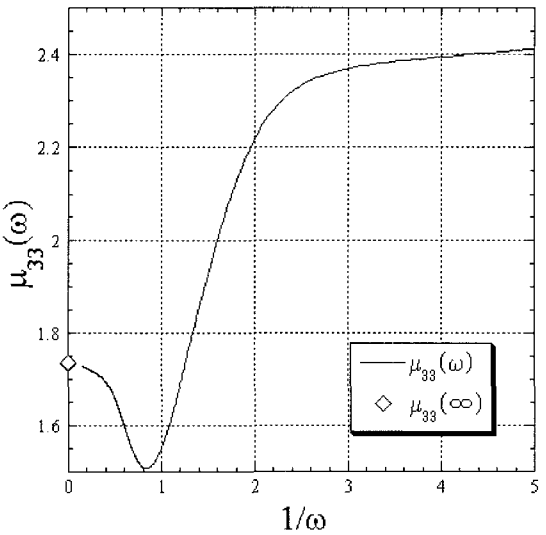

Fig. 5. Added mass at infinite frequency.

$\lambda_{33}(\omega)/\omega$ is sufficiently small, and thus it is assumed to be zero. As can be seen in Fig. 4, smaller the division number N, shorter the duration of the obtained $L_{33}(t)$ becomes. However, precision is almost the same regardless of the division number N. In the following calculations, $L_{33}(t)$ obtained for $N = 1024$ is used.

The added-mass at infinite frequency $\mu_{33}(\infty)$ is calculated by integrating Eq. (3) for the range up to $\omega = 2\pi$ instead of integrating up to $\omega = \infty$ by assuming $\lambda_{33}(\omega) = 0$ when $\omega > 2\pi$. The selection of ω_1 is known to be not so sensitive to the final result of $\mu_{33}(\infty)$ (see for example, Maeda *et al.*, 1991). Thus, we have chosen $\omega_1 = 2\pi$ for convenience, as we need not evaluate Cauchy principle value. As seen in Fig. 5, the value of $\mu_{33}(\omega)$ approaches the evaluated value of $\mu_{33}(\infty)$ as $1/\omega \to 0$. Thus, Fig. 5 validates the evaluation of $\mu_{33}(\infty)$.

4.2 Heaving Motion in Regular Waves

Heaving motion of the truncated circular cylinder in regular waves has been calculated by time-domain simulation. The equation of the motion is as follows:

$$\{m_{33}+\mu_{33}(\infty)\}\ddot{\zeta}_3(t)+\int_0^t L_{33}(\tau)\ddot{\zeta}_3(t-\tau)d\tau + K_{33}\zeta_3(t) = H_A X_3(\omega_1)\sin\omega_1 t \tag{11}$$

where ω_1, H_A and $X_3(\omega_1)$ refer to the circular frequency of the incident wave, the wave amplitude and the wave exciting force in heaving direction due to unit-amplitude incident wave, respectively. The values of $X_3(\omega_1)$ are evaluated beforehand by the eigenfunction expansion matching method in the frequency domain.

The Response Amplitude Operator (R.A.O.) of the heaving response in the frequency domain can be obtained as

$$R_3(\omega) = \frac{|\zeta_3(\omega)|}{H_A} = \left|\frac{iX_3(\omega)}{-\omega^2\{m_{33}+\mu_{33}(\omega)\}-i\omega\lambda_{33}(\omega)+K_{33}}\right| \tag{12}$$

where $\zeta_3(\omega)$ is the amplitude of the heaving response in the frequency domain and $R_3(\omega)$ is the R.A.O. of the heaving response.

Fig. 6 shows the result of the frequency domain analysis by Eq. (12) and the ones by the time series analysis by Eq. (11) at 10 distinct points corresponding to $\omega_1 = 0.1$, 0.6, 0.8, 0.9, 1.0, 1.1, 1.2, 1.4, 2.0 and 5.0. The steady state of the time-series response has been judged by plotting it in the graph. As can be seen in Fig. 6, both results agree very well, indicating that the time series analysis for sinusoidal steady excitation has been verified.

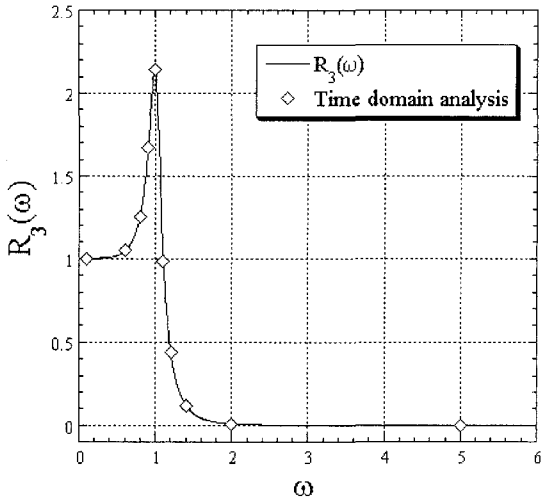

Fig. 6. R.A.O. of the heaving motion in regular waves.

4.3 Heaving Motion in Irregular Waves

Assuming that the incident wave consists of many sinusoidal waves of different frequencies with random phase angles, the time series of the irregular wave exciting force, $f_3(t)$, can be obtained form its power spectrum, $S_3(\omega)$, considering N components of regular waves:

$$f_3(t) = \sum_{k=1}^{N}\sqrt{2S_3(\bar{\omega}_k)\Delta\omega}\cos(\bar{\omega}_k t+\theta_k) \tag{13}$$

where

$\bar{\omega}_k = \dfrac{\omega_k+\omega_{k-1}}{2}$, $\Delta\omega = \omega_k - \omega_{k-1}$, θ_k: random numbers such as $0 \le \theta_k \le 2\pi$.

Furthermore, the power spectrum of the exciting force in the heaving direction, $S_3(\omega)$, can be obtained from the power spectrum of the wave, $S_3(\omega)$, and the exciting force for a unit amplitude of the wave, $X_3(\omega)$, as

$$S_3(\omega) = |X_3(\omega)|^2 S_0(\omega) \tag{14}$$

If the Bretschneider and Mitsuyasu's spectrum is used, it can be expressed in terms of the frequency, ω, the height of the significant wave, $H_{1/3}$, and the period of the significant wave, $T_{1/3}$, as

$$S_0(\omega) = 0.258\left(\frac{H_{1/3}}{gT_{1/3}}\right)^2 g^2\left(\frac{\omega}{2\pi}\right)^{-5}\exp\left\{-1.03\left(T_{1/3}\frac{\omega}{2\pi}\right)^{-4}\right\} \tag{15}$$

The time series response due to the irregular wave excitation given by Eq. (13) has been obtained by solving Eq. (1) by Newmark-β method. The verification of the time

series response is made by comparing their variances with the ones obtained by the frequency domain analysis. Here, the transient response part is omitted in the time series response results. The verifications have been made for non-dimensional period of the significant wave of $T_{1/3} = 4.5$, 7.0, and 16.0, each with $H_{1/3} = 1.0$.

Table 2 shows the comparisons between the variances σ_w^2 for the frequency-domain analysis and the ones σ_t^2 for the time-domain analysis. The duration for the time-domain analysis is taken for 255.6 seconds for all cases. As seen in Table 2, the variances for the time-domain analysis have different values for their different phases, θ_k. However, the average of the variances for the time-domain analysis coincides well with the corresponding one for the frequency-domain analysis. Thus, the response analysis of 1 D.O.F. system for the forced oscillation due to irregular waves has been verified. Also, Fig. 7 represents an example of the result for the case of $T_{1/3} = 7.0$.

Table 2. Variations of the heaving response due to irregular waves

	Significant Wave Period		
	$T_{1/3}$=4.5	$T_{1/3}$=7.0	$T_{1/3}$=16.0
$\sigma_t^2(\theta_1)$	0.794	0.459	0.0896
$\sigma_t^2(\theta_2)$	0.736	0.388	0.126
$\sigma_t^2(\theta_3)$	0.453	0.578	0.0736
$\sigma_t^2(\theta_4)$	0.717	0.430	0.110
$\sigma_t^2(\theta_5)$	0.777	0.323	0.116
$\sigma_t^2(\theta_6)$	0.440	0.402	0.0986
$\sigma_t^2(\theta_7)$	0.712	0.584	0.108
$\sigma_t^2(\theta_8)$	0.564	0.508	0.838
$\sigma_t^2(\theta_9)$	0.898	0.376	0.140
$\sigma_t^2(\theta_{10})$	0.554	0.645	0.0838
Average of σ_t^2	0.665	0.470	0.103
σ_ω^2	0.617	0.433	0.101
Error	7.76×10^{-2}	8.40×10^{-2}	2.56×10^{-2}

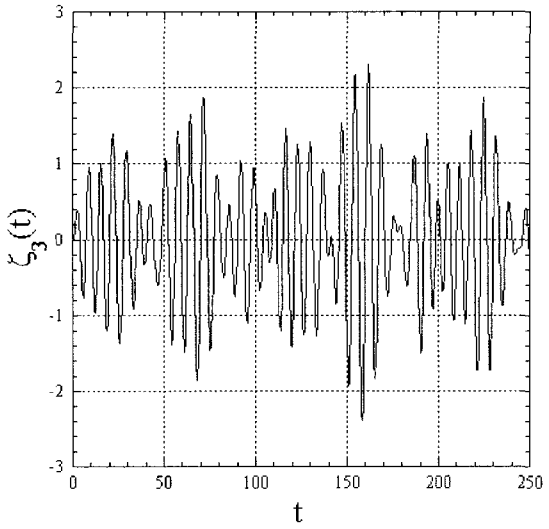

Fig. 7. Time series of the heaving motion in irregular waves.

5. Surge, Heave, and Pitch Motion of a Moored Floating Body

Time domain analysis as a 3 D.O.F. system (Surge, Heave, and Pitch motions) is made for the same analytical model as before (circular cylinder with $D = 0.5$) located in the infinite depth water. The linear spring in surge direction is considered as a model of the mooring system.

5.1 Coefficients of the Matrices

The matrix for the memory effect function, $[L_{ij}(t)]$, and the added-mass matrix at the infinite frequency, $[\mu_{ij}(\infty)]$, can be obtained by the same procedure as before.

The mass matrix $[m_{ij}]$ is given as

$$[m_{ij}] = \begin{bmatrix} m & 0 & 0 \\ 0 & m & 0 \\ 0 & 0 & mr^2 \end{bmatrix} \tag{16}$$

where non-dimensionalized mass of the floating body is $m = 0.5\pi$, and the non-dimensionalized moment of inertia is $m^2 = 0.18\pi$, where the radius of gyration is assumed as $r = 0.6a$ ($a = 1.0$).

The restoring force coefficient matrix $[K_{ij}]$ is given by

$$[m_{ij}] = \begin{bmatrix} K_{11} & 0 & 0 \\ 0 & K_{33} & 0 \\ 0 & 0 & K_{55} \end{bmatrix} \tag{17}$$

$$K_{33} = A = \pi, \quad K_{55} = mg\overline{GM}/\rho g a^4 \tag{18}$$

Here, the meta-center height $\overline{GM}$ may be calculated from $\overline{GM} = \overline{BM} + \overline{KB} - \overline{KG}$, where G represents the center of mass, M the meta-center, B the center of buoyancy, and K the keel (bottom of the floating body); $\overline{BM} = I_y/\nabla$ (∇: the displaced volume, I_y: the second moment of the water-plane area), $\overline{KB} = D/2$, and $\overline{KG} = D$ are assumed. Substituting $I_y = \pi a^4/4$ and $\nabla = \pi a^2 D$ into Eq. (18), one obtains $K_{55} = 0.125\pi$. The linear spring constant K_{11} represents the non-dimensionalized mooring stiffness, and is given arbitrarily in the following numerical calculations.

5.2 Time-domain Response Simulation Due to Regular Waves

Time-domain response simulation due to regular waves has been made. The results of the response are compared with the ones by the frequency domain analysis. Fig. 8

shows the comparison of the R.A.O. for surge response at the excitation angular frequencies of $\omega_1 = 0.1$, 0.4, 0.5, 0.6, 0.7, 0.8, 1.0, 1.5, 2.5, and 3.5, respectively. The spring constant for the mooring is assumed as $K_{11} = 0.1$. The steady state response has been observed after t=50 in all these cases, where the envelope function for the incident wave elevation is employed until t=20. As can be seen in Fig. 8, good agreement is observed between the results by the time-domain simulation program and the ones by the frequency domain analysis. Then, the spring constant for the mooring is varied as $K_{11} = 0.01$ and $K_{11} = 1.0$. The result of the surge response for each case when $\omega_1 = 0.4$ is shown in Figs. 9 and 10. In Fig. 9, one observes the transient response component at low frequency region, corresponding to the long natural period in the surge direction. Such a low frequency oscillation is very important for mooring design; thus, the time-series analysis considering the memory effect may be effectively used for mooring design purposes.

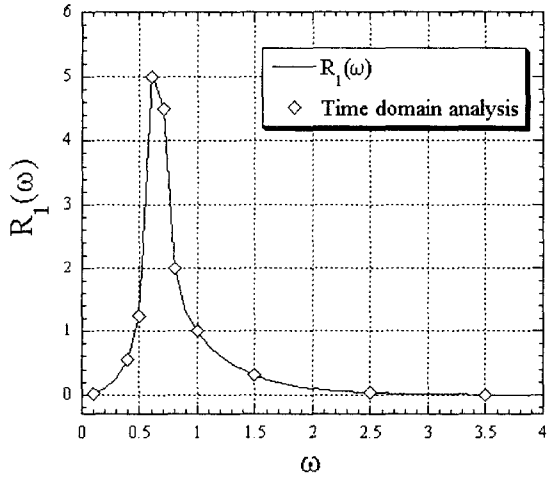

Fig. 8. R.A.O. of the surging motion in regular waves (K_{11}=0.1).

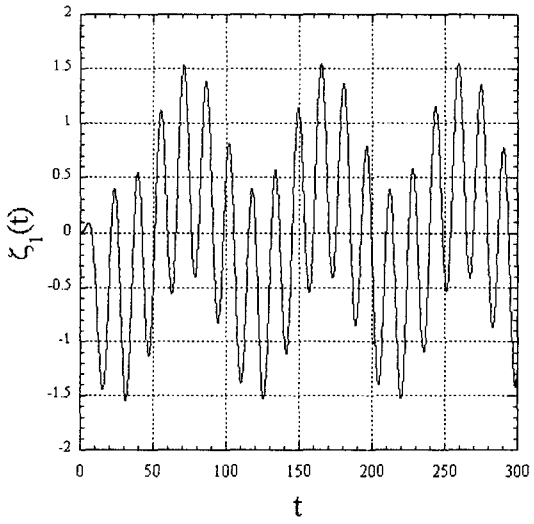

Fig. 9. Time series of the surging motion in regular waves (ω_1=0.4, K_{11}=0.01).

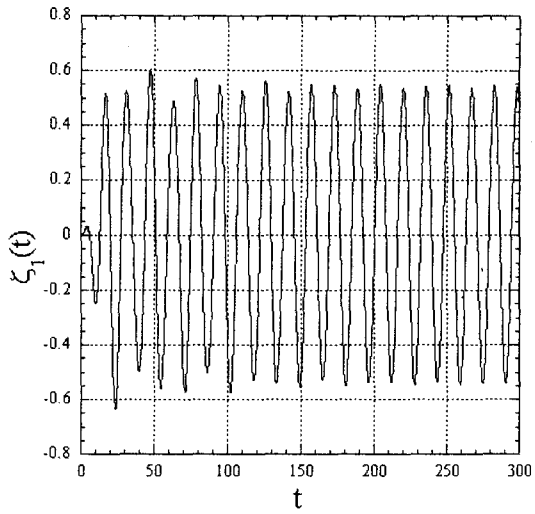

Fig. 10. Time series of the surging motion in regular waves (ω_1=0.4, K_{11}=1.0).

6. Conclusions

The time-domain response simulation program of floating bodies considering the memory effect function has been developed. The numerical results have been compared with the results by Newman (1985), and also with the ones obtained by the frequency domain analysis. Through the comparisons, the developed program has been verified to be accurate. In the proposed method, the inverse Fourier transform of the radiation damping coefficients into the memory effect function has been made directly by utilizing the FFT (Fast Fourier Transform), and the time-domain simulation has been made by Newmark-β method. The most advantageous point of this study would be the acceleration of the computation time in order to obtain the memory effect function. In the former studies, it is reported that the computation time for memory effect function is very time consuming (Kashiwagi, 2000). The efficiency of the proposed methodology has been confirmed by numerical examples.

References

Cummins WE (1962) The impulse response functions and ship motion, Schiffstechnik, 9: 101-109.

Endo H, Yago K (1991) Time history response of a large floating structure subjected to dynamic load, J. Soc. Naval Architects Japan, 186: 369-376.

Kashiwagi M (2000) A time-domain mode-expansion method for calculating transient elastic responses of a pontoon-type VLFS, J. Marine Science and Technology, 5: 89-100.

Lwin MM (2000) Floating bridges, Bridge Engineering Handbook (eds. Chen WF, Duan L), CRC Press, Chap 22.

Maeda H, Jo HJ, Miyajima S (1991) A study on the stability of semi-submersible rig in multi-directional waves, J. Kansai Soc. Naval Architecture, 215: 113-121.

Maruyama T, Watanabe E, Utsunomiya T, Tanaka H (1998) A new movable floating bridge in Osaka Harbor, Proc. of the 6th East Asia-Pacific Conference on Structural Engineering & Construction, Taiwan, 429-434.

Newman JN (1985) Transient axisymmetric motion of a floating cylinder, J. Fluid Mech., 157: 17-33.

Newmark NM (1959) A method of computation for structural dynamics, J. Eng. Mech., ASCE, 85: 67-94.

Takagi M, Arai S (1996) Wave response theory of ships and offshore structures, seizando, Japan.

Teng B, Taylor RE (1995) New higher-order boundary element methods for wave diffraction/radiation, Applied Ocean Research, 17: 71-77.

Yeung RW (1981) Added mass and damping of a vertical cylinder in finite-depth waters, Applied Ocean Research, 3: 119-133.